HHS Public Access

Author manuscript

Biochim Biophys Acta Gen Subj. Author manuscript; available in PMC 2024 February 01.

Published in final edited form as:

Biochim Biophys Acta Gen Subj. 2023 February ; 1867(2): 130284. doi:10.1016/j.bbagen.2022.130284.

UBQLN2 undergoes a reversible temperature-induced conformational switch that regulates binding with HSPA1B: ALS/FTD mutations cripple the switch but do not destroy HSPA1B binding

Trong H. Phung[1,2], **Micaela Tatman**[1,2], **Mervyn J. Monteiro**[1,2,*]

[1]Center for Biomedical Engineering and Technology, University of Maryland School of Medicine, Baltimore, Maryland, United States of America

[2]Department of Anatomy and Neurobiology, University of Maryland School of Medicine, Baltimore, Maryland, United States of America

Abstract

Here we present evidence, based on alterations of its intrinsic tryptophan fluorescence, that UBQLN2 protein undergoes a conformational switch when the temperature is raised from 37°C to 42°C. The switch is reset on restoration of the temperature. We speculate that the switch regulates UBQLN2 function in the heat shock response because elevation of the temperature from 37°C to 42°C dramatically increased *in vitro* binding between UBQLN2 and HSPA1B. Furthermore, restoration of the temperature to 37°C decreased HSPA1B binding. By comparison to wild type (WT) UBQLN2, we found that all five ALS/FTD mutant UBQLN2 proteins we examined had attenuated alterations in tryptophan fluorescence when shifted to 42°C, suggesting that the conformational switch is crippled in the mutants. Paradoxically, all five mutants bound similar amounts of HSPA1B compared to WT UBQLN2 protein at 42°C, suggesting that either the conformational switch is not instrumental for HSPA1B binding, or that, although damaged, it is still functional. Comparison of the poly-ubiquitin chain binding revealed that WT UBQLN2 binds more avidly with K63 than with K48 chains. The avidity may explain the involvement of UBQLN2 in autophagy and cell signaling. Consistent with its function in autophagy, we found UBQLN2 binds directly with LC3, the autophagosomal-specific membrane-tethered protein. Finally, we provide evidence that WT UBQLN2 can homodimerize, and heterodimerize with WT

*Corresponding author. monteiro@som.umaryland.edu, Tel: 410-706-8132, FAX: 410-706-8184.

Author Contributions

All the authors designed, performed, wrote and/or edited the paper.

Consent for publication

All authors read and approved the manuscript.

Competing Interests

The authors declare no competing interests.

Declaration of interests

The authors declare that they have no known competing financial interests or personal relationships that could have appeared to influence the work reported in this paper.

UBQLN1. We show that ALS mutant P497S-UBQLN2 protein can oligomerize with either WT UBQLN1 or 2, providing a possible mechanism for how mutant UBQLN2 proteins could bind and inactivate UBQLN proteins, causing loss of function.

Graphical Abstract

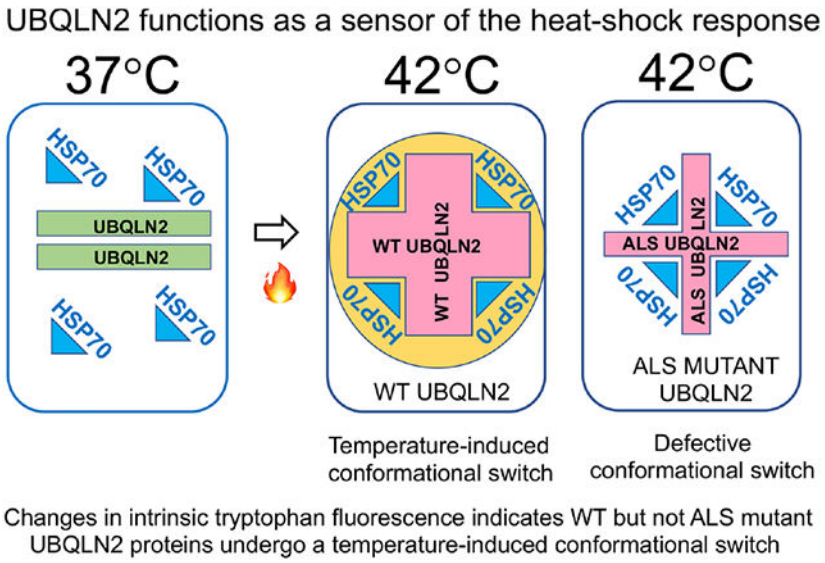

Keywords

Amyotrophic lateral sclerosis; UBQLN2; HSPA1B; ubiquitin chains; intrinsic tryptophan fluorescence

Introduction

Mutations in UBQLN2, an intronless gene on the X chromosome, are linked to a spectrum of neurodegenerative disorders, most notably amyotrophic lateral sclerosis (ALS) and frontotemporal dementia (FTD) [1-3]. The UBQLN2 open reading frame encodes (ORF) a 624 amino acid (aa)-long protein. It is one of five related UBQLN proteins found in humans [3, 4]. UBQLN proteins are distinguished by possessing both a ubiquitin-like (UBL; ~70 aa) and a ubiquitin associated (UBA; ~45 aa) domain at their N- and C-terminus, respectively, which are separated by a long linker region containing a variable number of additional domains [3]. All UBQLN proteins contain two closely-spaced STI1 domains in the linker region, but UBQLN2 is unique in possessing an additional insert of 12 tandem PXX repeats, whose function is not known. Interestingly, most missense mutations that cause ALS/FTD map in or around the PXX domain [2, 3].

UBQLN proteins predominantly function as guardians of proteostasis (reviewed by [5]) by performing various protein quality control functions, such as shuttling misfolded proteins to the proteasome for degradation. Their two end domains play instrumental roles in this function. The UBA domain binds polyubiquitin chains that tag misfolded proteins, whereas the UBL domain interacts with subunits in the 19S cap of the proteasome. UBQLN proteins

also function in autophagy, both by acting as a receptor for packaging ubiquitinated cargo into autophagosomes and for promoting endosome/lysosomal acidification [6-9]. The UBA is most likely responsible for binding the ubiquitinated cargo, but it remains uncertain how different UBQLN isoforms localize to autophagosomes. UBQLN1, 2 and 4 isoforms have all been detected in the organelle, yet only UBQLN4 is known to directly bind to LC3, the main autophagosome receptor, leaving the manner of how other UBQLN proteins are recruited to autophagosomes unsettled [6, 7, 9, 10].

Although UBQLN proteins target terminally misfolded proteins for degradation, there is accumulating evidence that they can also engage in protein refolding, either independently or with other factors (reviewed by [5]). This refolding activity has been attributed to its STI1 domains. STI1 domains bind heat shock proteins, which are chiefly responsible for refolding proteins in cells [11, 12]. Indeed, there is good evidence that UBQLN2 binds HSP70-like proteins and that ALS/FTD mutations in UBQLN2 reduce this binding [13-17]. However, most of these findings have been conducted using whole cell lysates, leaving irresolution whether it stems from an alteration in direct binding of the proteins.

Here we report on differences in the *in vitro* binding properties of UBQLN2 proteins with a variety of its putative substrates, including HSPA1B, polyubiquitin chains, LC3 and UBQLN1. We show that a shift in temperature from 37°C to 42°C alters the binding of some of these proteins, particularly a dramatic increase in HSPA1B binding. We provide evidence that the 5°C shift in temperature induces a change in the conformation of WT UBQLN2 based on a significant shift in the wavelength and intensity of its intrinsic tryptophan fluorescence. Interestingly, all five ALS/FTD mutant UBQLN2 proteins tested failed to manifest the spectral shift, suggesting that they are misfolded. Despite this difference, the mutant proteins still displayed a similar temperature-dependent increase in HSPA1B binding as compared to WT UBQLN2 protein. We also provide biochemical evidence that UBQLN2 protein can homodimerize as well as heterodimerize with UBQLN1. We discuss the implications of these findings in relation to the possible mechanisms by which UBQLN2 mutations may induce disease.

Materials and Methods

Cloning, expression, and purification of recombinant proteins

A cDNA encoding the complete human HSPA1B ORF was cloned between the NdeI and XhoI site in the bacterial pET-21a expression vector to express full-length (FL) HSPA1B tagged at its C-terminus with 6 His residues. Sub-constructs expressing the ATP- (1 to 385 aa) and peptide- (Pep) binding domains (386 to 641aa) of HSPA1B with 6 His tags were also generated, using a similar cloning strategy. cDNAs encoding the complete human ORF for WT UBQLN2 protein, or carrying any of the P497H, P497S, P506T, P509S or P525S ALS mutations [1] were cloned between the BamHI and XhoI sites in pET45b to express different FL UBQLN2 proteins with 6 His residues at their N-terminus. An identical set of N-terminal GST-tagged versions for all the UBQLN2 constructs were also made, as described previously [18]. WT UBQLN2 ORF was also cloned between the BamHI and HindIII sites in pMAL-c2X to express UBQLN2 with the maltose binding protein E (MBP) at its N-terminus. The placement of the protein-purification tags at the N-terminus

of UBQLN2 was done to avoid steric interference of the UBA domain that is located at the C-terminus and which is known to be involved in ubiquitin binding, which was a subject of our investigations. The complete LC3B ORF was cloned between the KpnI and XhoI sites in pET45b to express LC3B with 6 His residues at its N-terminus. All of the clones were sequenced and verified to encode the appropriate recombinant fusion proteins.

All the pET plasmids were transformed into Rosetta (DE3) bacteria whereas the GST plasmids were transformed into DH5α bacteria. Bacterial cultures for all the clones were grown with constant agitation (200 RPM) at 37°C overnight and then induced with 0.5-1 mM IPTG at 30°C for 4 hours. Bacteria were harvested by centrifugation at 4°C, 4,000 RPM, for 10 minutes. The pellets were then used for purification. The bacterial pellets were resuspended in lysis buffer (50 mM Tris pH 8.0, 300 mM NaCl, and 5% glycerol) and lysed with 5 mg/ml lysozyme. To prevent protein breakdown, the lysates were also treated with one proteinase inhibitor cocktail tablet (#11836170001 Sigma-Aldrich, St. Louis, MO, USA) and a small amount of pefabloc (#ALX-270-022-G001, Enzo Life Science, Farmingdale, NY, USA). Then, lysates were sonicated twice at 35% duty cycle and 2 ¾ output for 2 minutes with a Branson Sonifier 450. The lysates were centrifuged at 20,000 RPM, 10°C for 20 minutes and the resulting supernatant was added to glutathione sepharose, Ni-NTA agarose, or amylose resin and rotated at 4°C for 4 hours before elution with 10 mM reduced glutathione, 250 mM imidazole, or 10 mM maltose, respectively through a gravity column. Finally, these purified recombinant proteins were dialyzed against dialysis buffer (20 mM Tris pH 8.0, 150 mM NaCl, and 10% glycerol), their protein concentrations were measured using the BCA assay, and they were stored at −80°C until required.

GST- and His-pulldown assays

For heat-induced binding assays: GST- or His-tagged proteins (2.8 μg GST, 10 μg GST-WT or mutant UBQLN2) were rotated with ligand proteins (at a molar equivalent to UBQLN1 or 2; includes K48 and K63 poly-ubiquitin (1-7) chains (Boston Biochemical#UC-240 and UC-340, respectively), and HSPA1B-His FL, HSPA1B ATP-His, HSPA1B Pep-HIs) in 1 ml binding buffer (20 mM Tris pH 8.0, 150 mM NaCl, 10% glycerol, and 0.1% NP-40) at 37°C or 42°C for 2 hours. Then 100 μl glutathione beads or Ni-NTA beads was added, and these protein/bead mixtures were rotated for 2 hours at 37 or 42°C. The beads were washed three times in pre-warmed binding buffer, resuspended in 100 mM Tris, pH 6.8, and then stripped of protein by addition of gel loading buffer with SDS [19] and boiling at 95-100°C for 5 min.

For non-heat induced binding assays: GST- or His-tagged proteins (2.8 μg GST, 10 μg GST-WT, or mutant UBQLN1 or 2) were rotated with ligand proteins (at a molar equivalent to UBQLN1 or 2; includes His-LC3) in 500 μl binding buffer 2 (20 mM Tris pH 8.0, 300 mM NaCl, 10% glycerol) at 4°C for 1 hour. Glutathione beads or Ni-NTA beads were pre-washed with sterile dH2O and incubated with 5% milk for 30 min. Then 50 μl of these blocked beads were added, and this protein/bead mixture was rotated for 30 min at 4°C. The beads were washed three times in binding buffer 2 with 0.1% NP-40 or Triton X-100, resuspended/washed in 100 mM Tris, pH 6.8, and then stripped of protein by adding gel loading buffer with SDS and boiling at 95-100°C for 5 min [19].

All pulldown samples were resolved by SDS-polyacrylamide gel electrophoresis (PAGE) and analyzed by either Coomassie Blue staining or immunoblotting [9].

Antibodies

The subsequent primary antibodies were used to verify correct protein expression and analyze GST-pulldown assays by immunoblot analysis. 6xHis-tagged recombinant proteins were detected with a mouse monoclonal anti-His antibody (#MA1-135 ThermoFisher Scientific, Waltham, MA, USA). The GST tag alone and GST-tagged proteins were detected with an in-house rabbit anti-GST antibody (UM-110). The maltose-binding protein tag was detected with a rabbit-antibody (#PA1-989, ThermoFisher Scientific). UBQLN2 was also detected with a mouse monoclonal anti-UQBLN2 antibody (#NBP2-25164, Novus Biologicals Centennial, CO, USA). Horseradish peroxidase-conjugated anti-mouse and anti-rabbit secondary antibodies were then used to detect binding of the primary antibodies by chemiluminescence [9].

Circular Dichroism Measurements

Circular dichroism (CD) spectra were measured using a Jasco J-810 spectropolarimeter connected to a temperature-regulated water bath. Triplicate measurements at 0.1 nm intervals from 190 to 250 nm wavelength were made of either the buffer alone (10 mM sodium phosphate (pH 7.5), 100 mM NaF) or of the different UBQLN2 proteins (~2 μM) diluted in the same buffer in a quartz cuvette with path length of 0.1 cm at 37°C and then at 42°C. The 42°C measurements were done after raising the temperature for the same protein mixture that were first measured at 37°C.

Intrinsic Tryptophan Fluorescence Assay

His-UBQLN2 (4 μg/μl) was incubated in 0, 1, 2, 3, 4 and 5 M guanidine hydrochloride (GndHCl) in phosphate buffered saline (PBS) solution for 2 hours in a 96 well plate, covered at 37°C. The plate was moved into Spectramax Gemini plate reader (Molecular Devices, LLC, San Jose, CA, USA) blanked with the respective concentrations of guanidine hydrochloride in PBS at 37°C and the fluorescence read over the entire 300 to 450 nm emission spectrum with fixed excitation at 270 nm. These steps were repeated on a separate plate with the same parameters at 42°C. The protocol was repeated at least three times per temperature and the data presented is the average curve of three measurements.

Serial and Single Column Assays

GST-, His-, and MBP-UBQLN2 were added in a 1:1:1 ratio, 100 μg each to a total volume of 500 μl. This protein mixture was denatured by the addition of 5 M GndHCl, and then gradually serially dialyzed in decreasing concentrations of GndHCl to 0 M GndHCl in dialysis buffer at 4°C, and then allowed to dialyze here overnight at 4°C. The following day, the protein mixture was incubated with 500 μl glutathione sepharose for 1 hour at 4°C. At room temperature, the bead and protein mixture were added to a gravity-flow column, washed 3 times with 1 ml dialysis buffer and twice eluted with1 ml of 10 mM reduced glutathione. The eluted fractions from the glutathione column were then transferred to the Ni-NTA column, followed by a similar incubation and elution with imidazole. GST-

UBQLN1 and His-UBQLN2 proteins were mixed in a 1:1 ratio and the denaturation, renaturation, bead-binding and elutions were conducted essentially as described above, except that protein binding was with Ni-NTA beads and elution was with imidazole. The flow-through and several of the eluted fractions were separated by SDS PAGE and analyzed by immunoblotting.

Statistical Analysis

All the data were analyzed using GraphPad Prism 9.3.1 software (GraphPad Software Inc, San Diego, CA), which was used to conduct student's t-test and one- and two-way ANOVA tests with the following P values used for the different values of significance. *$P < 0.05$, **$P < 0.01$, ***$P < 0.001$, ****$P < 0.0001$.

Results

A shift in temperature from 37°C to 42°C increases HSPA1B binding with UBQLN2

Previous studies had shown that binding of HSP70-related proteins with UBQLN2 is increased at 42°C compared to 37°C [13], but whether this arises from a change in direct binding was not known. To examine this, we conducted GST-pulldown assays comparing binding at 37°C and 42°C of recombinantly expressed and purified His-tagged human HSPA1B protein to GST-tagged wild type (WT) human UBQLN2. HSPA1B, which is 100% identical to HSPA1A in protein sequence, was used for our investigations as HSPA1A/B proteins have been recovered as binding partners of UBQLN2 [13, 15, 16]. The purity of the purified proteins used in the assays is shown in Supplemental Fig S1. The GST-pulldown assays revealed an approximately 14-fold increase in HSPA1B binding with GST-WT-UBQLN2 at 42°C compared to 37°C (Fig 1A and B). Binding at 37°C with GST-WT-UBQLN2 was marginally greater than with GST alone, which we used as a negative control.

To map the UBQLN2 binding site in HSPA1B we subdivided the protein into two portions, testing both the N-terminal ATP-binding and the C-terminal peptide-binding domains [20] for UBQLN2 binding. The GST-pulldown assays revealed that the temperature-induced increase in UBQLN2 binding occurs primarily with the HSPA1B ATP-binding and not its peptide-binding domain (Fig 1C and D). Negligible binding was observed with the peptide-binding domain with either GST-UBQLN2 or GST alone, at both 37°C and 42°C.

The heat-induced increased in HSPA1B binding with UBQLN2 is reversible

We next examined whether the heat-induced binding between HSPA1B and UBQLN2 is reversible. To do so, we conducted three parallel sets of GST-pulldown assays, in which HSPA1B was incubated with either GST-WT-UBQLN2 or GST alone. Two-hour incubation periods were conducted at either, 37°C, 42 °C, or with a temperature shift from 42°C for 1 hour to 37°C for another hour for the third sample. Analysis of HSPA1B binding by immunoblotting revealed an increased binding of HSPA1B with GST-WT-UBQLN2 but not with GST alone when incubated at 42°C only (Fig 1E and F). Importantly, the amount of HSPA1B that was bound to GST-WT-UBQLN2 when shifted back from 42°C to 37°C was

similar to that of unshifted 37°C mixtures. These results suggest that HSPA1B binding with UBQLN2 is heat-reversible.

GST-UBQLN2 proteins carrying ALS/FTD mutations display similar temperature-induced binding with HSPA1B as WT-UBQLN2

We next tested whether UBQLN2 proteins carrying ALS/FTD mutations have altered HSPA1B binding using similar GST-pulldown assays. For these assays, we used recombinant purified GST-UBQLN2 fusion proteins carrying each of the five different missense UBQLN2 mutations (P497H, P497S, P506T, P509S and P525S) genetically linked to ALS or ALS/FTD that were identified by Deng et al. [1]. Analysis of these proteins by SDS-PAGE and Coomassie Blue staining revealed they were of the expected size for the intact GST-UBQLN2 proteins and were more than 90% pure (Fig S1). The GST-pulldown results using the proteins revealed all five UBQLN2 mutants had similar increases in HSPA1B binding between 42°C and 37°C compared to WT-UBQLN2 (Fig 2A and B). Some mutants displayed slightly lower binding with HSPA1B than WT-UBQLN2, but the changes were not significant (Fig 2B). These results suggest that the five ALS/FTD mutations we studied do not significantly alter the temperature-induced increase in binding of HSPA1B with UBQLN2.

A raise in temperature from 37°C to 42°C induces a conformational change in UBQLN2 structure

We next investigated the possible reason for the thermal-induced increase in HSPA1B binding with UBQLN2, speculating that the 5°C shift in temperature induces a conformational change, exposing binding sites in one or both proteins. To determine whether UBQLN2 undergoes such a conformational change, we measured its intrinsic tryptophan (Trp) fluorescence at 37°C and 42°C. A shift in the spectral peak of Trp fluorescence, and sometimes its intensity, is widely used to detect conformational changes in proteins. UBQLN2 contains one Trp residue at position 320, which is almost in the middle of the protein (see [5]). Although the structure of UBQLN2 has not been solved, the presence of the sole Trp residue provides a convenient tool for using alterations in Trp fluorescence for reporting on alterations in UBQLN2 folding.

We first assessed the utility of the method by measuring alterations in Trp fluorescence of lysozyme before and following incubation with increasing concentrations of guanidine hydrochloride (GndHCl), which is a known denaturant (Fig S2). The spectral peak of Trp fluorescence for lysozyme is known to increase by approximately 5 nm following its denaturation. For all the scans, the excitation was fixed at 270 nm, and the emission spectra of the samples was collected at 2 nm intervals from 300 to 450 nm (Fig S2). As expected, the spectral peak of Trp fluorescence for lysozyme increased progressively with increasing GndHCl concentration, consistent with progressive denaturation of the protein and exposure of its Trp residue to the aqueous environment.

We applied the same methodology to determine whether the Trp fluorescence for WT-UBQLN2 differed at 37°C and 42°C. For this analysis, and subsequent analysis of the mutants, we used six His-tagged-UBQLN2 purified proteins, as the prior GST-tag has a

Trp residue whose signal could have complicated interpretation of the results. A Coomassie Blue stained gel of the purified proteins is shown in Fig S1, demonstrating the WT and five UBQLN2 proteins had similar purity.

The spectral scans for His-WT-UBQLN2 at 37°C and 42°C revealed a significant increase in both the peak wavelength and the intensity of Trp fluorescence at the higher temperature, consistent with the idea that the higher temperature induces a conformational change in UBQLN2 structure (Fig 3A to C). The alterations are better visualized by examining the more refined 330 to 350 nm wavelength portion of the spectral scans (Fig S3A).

We next compared the spectral scans collected at 37°C and 42°C for each of the five UBQLN2 mutants, but found no significant difference in either the peak wavelength or intensity of Trp fluorescence following the shift in temperature for any of them (Fig 3A to C). A slight increase in the peak wavelength of fluorescence was seen for the P506T mutant (Fig S3A), but the change was not significant. Slight increases in the intensity of Trp fluorescence was seen for all the mutants, except the P497S mutant, but none of the differences were statistically significant (Fig 3C).

We next examined whether the temperature-induced changes in Trp fluorescence seen for WT-UBQLN2 are reversible by shifting the temperature of the protein from 42°C back to 37°C. Indeed, the spectral scans showed that the peak wavelength of Trp was reduced when returned to 37°C, demonstrating the conformational change is tunable by temperature (Fig 3D and S3B).

Comparison of the structural properties of WT and ALS mutant UBQLN2 proteins by CD and Trp fluorescence following chemical denaturation suggests ALS mutant UBQLN2 proteins are not grossly misfolded

The preceding results suggests that WT-UBQLN2 protein is dynamic, in that its conformation is switchable by a temperature change from 37°C to 42°C, whereas the ALS mutant proteins are crippled in this capability. We investigated whether the temperature-induced conformational switch can be monitored by CD. This structural assay could also reveal if the mutant proteins are grossly misfolded. To complement these assays, we also conducted Trp fluorescence experiments to determine whether WT and mutant UBQLN2 proteins exhibit different sensitivity to denaturation with increasing concentrations of GndHCl.

CD measurements were conducted for the WT and all five ALS mutant UBQLN2 proteins at 37°C, and then immediately for the same mixtures after raising the temperature to 42°C. The scans revealed no noticeable difference between the scans at the two temperatures, for any of the proteins (Fig S4). The results suggest that the change in Trp fluorescence identified for WT UBQLN2 is subtle and does not involve gross alteration in protein structure. Furthermore, the profile of the scans for the WT and ALS mutant proteins were very similar suggesting the mutant proteins are not grossly misfolded (Fig S4H). This finding is consistent with the same conclusion reached in an independent study [13].

The results of the Trp fluorescence scans performed at 37°C after incubation of the different UBQLN2 proteins in increasing concentrations of GndHCl from 0 to 5M is shown in Figure 4. The spectral scans show a progressive increase in the wavelength of peak Trp fluorescence for all the UBQLN2 proteins examined, with the greatest shift (>10 nm) observed when the proteins were incubated with the highest 5M GndHCl concentration (Fig 4A and B). The scans also revealed a progressive decrease in the intensity of Trp fluorescence after incubation with increasing GndHCl concentrations up to 4M, followed by a slight increase after incubation with 5M GndHCl (Fig 4A and C). However, when compared to WT UBQLN2 protein, none of the changes in either the shift in wavelength or the alteration in intensity of peak Trp fluorescence were different between the WT and any of the mutant UBQLN2 proteins. Subtle differences were found for each of the mutants, which may represent unique characteristics of protein folding/unfolding of the proteins.

In summary, the CD and chemical denaturation experiments strongly suggest that the ALS mutant UBQLN2 proteins studied here are not grossly misfolded compared to WT UBQLN2, suggesting that the temperature-induced Trp fluorescence change we identified for the WT protein as potentially significant.

Preferential binding of UBQLN2 with K63-polyubiquitin chains

We previously showed UBQLN1 binds more strongly with K63-linked polyubiquitin chains than with K48 chains [21]. To examine the ubiquitin chain binding specificity of UBQLN2, we conducted pulldown experiments with WT-UBQLN2 and the same two sets of polyubiquitin chains at both 37°C and 42°C. The K48 and K63 chains used in these assays are composed of a mixture of single and multiple ubiquitin chain-linked moieties (single ubiquitin moiety (Ub1), Ub2, Ub3, Ub4, Ub5, Ub6, and Ub7 moieties distinguishable by their separation on the SDS-PAGE gels with molecular weights of ~9, 17, 26, 34, 43, and 52 kDa, respectively, Fig 5A). Despite the addition of similar concentrations of the chains, the beads containing His-tagged WT-UBQLN2 protein bound approximately 10-fold more K63 chains than K48 chains (Fig 5A and B). Interestingly, binding was mainly with ubiquitin chains that were 4 or longer and negligible with chains that were 3 and shorter for both K63 and K48, suggesting UBQLN2 binds preferentially to longer poly-ubiquitin chains. By comparison, there was only faint binding of both chains with the empty pulldown beads, demonstrating the specificity of the UBQLN2 bindings. Interestingly, the amount of the chains that were bound with UBQLN2 at 42°C was slightly reduced compared to at 37°C, but the difference was not significant (Fig 5B).

We next examined whether the five ALS mutant UBQLN2 proteins have alterations in the ubiquitin chain binding. Repetition of the pulldown assays using all five UBQLN2 mutants revealed only minor differences in K63 ubiquitin chain binding compared to WT-UBQLN2 protein, for both 37°C and 42°C incubations (Fig 5D and E). Interestingly, all the UBQLN2 proteins, including the WT and mutants had slightly lower binding of K63 chains at 42°C compared to 37°C, but the differences were not significant (Fig 5E). A similar comparison of K48 chain binding revealed a similar trend of decreased binding of the chains at 42°C compared to 37°C. Most of these differences were not significant, with the exception of the P506T mutant (Fig 5C and E). The P506T mutant displayed increased binding with K48

chains at both 37°C and 42°C compared to WT-UBQLN2 (Fig 5C and E). Please note, that the blots for the K48 and K63 bindings cannot be compared with one another as their exposures are different.

Taken together these results indicate that UBQLN2 binds preferentially with K63 ubiquitin chains than with K48 chains. The results also show that the five UBQLN2 mutants studied here have similar K63 ubiquitin binding capability, but that one of them in particular, the P506T mutant, differs from the WT protein in having increased binding with K48 ubiquitin chains.

Evidence that UBQLN2 binds directly to LC3

Proteins that are tagged with K63 polyubiquitin chains are typically, but not exclusively, targeted for degradation by autophagy [22, 23]. We previously showed UBQLN2 functions in autophagy, including a visual demonstration of its presence in autophagosomes [9]. However, the process by which UBQLN2 gets recruited to autophagosomes was not known. We conducted pulldown assays to examine the possibility that UBQLN2 recruitment to autophagosomes is through direct binding with LC3, the autophagosome specific protein. Accordingly, purified His-tagged LC3 protein was incubated with either GST-WT-UBQLN2 or with GST alone and binding of LC3 was assessed by immunoblots. The results show that LC3 was pulled-down by WT-UBQLN2 but not by GST alone, demonstrating that UBQLN2 can bind directly with LC3 (Fig 6).

UBQLN2 forms homodimers and can heterodimerize with UBQLN1

Considerable evidence suggests that dominant mutations in UBQLN2 cause disease through both loss- and gain-of-function mechanisms. However, it is unknown how mutations induce loss of function. Here we explored the possibility that mutant UBQLN2 protein binds and possibly inactivates other UBQLN isoforms, including expression of WT-UBQLN2 protein encoded in females by the non-mutated allele, through multimerization of the proteins.

We conducted sequential pulldown assays to determine whether UBQLN2 is capable of multimerization. In this assay, GST-, His- and MBP-tagged WT-UBQLN2 purified proteins were mixed in approximately 1:1:1 molar ratio, and binding between the proteins was analyzed by immunoblotting following sequential application and elution over GST-agarose and Ni-NTA agarose containing columns (Fig 7). For these assays, the proteins were first denatured with 5M GndHCl in order to separate any potential homo-oligomerization of the proteins. The GndHCl solution was then slowly removed by dialysis to allow protein-protein interactions. Monitoring of native and renatured WT UBQLN2 following this same procedure revealed they had similar CD spectra, suggesting that the protein used after renaturation has similar structure as the native protein (Fig S4A). Immunoblots of representative fractions, including the proteins before mixture, after mixture, and after flow-through and elution from the columns is shown in Figures 7A and B. The immunoblots of the initial mixture when probed with an anti-UBQLN2 specific antibody revealed three products with distinct sizes, consistent with fusion of the three different size tags with UBQLN2 (His < GST < MBP) (Fig 7A). Note some of the fusion proteins contained some breakdown products, but their identity was confirmed by immunoblotting (see below

Fig 7B and D). All three fusion proteins were recovered in the glutathione (GSH) eluates following passage of the mixture over the first GST-agarose column, suggesting either all three proteins had oligomerized, or that each had individually oligomerized with the GST-tagged protein (Fig 7A). However, when this eluate was applied over the Ni-NTA column, only the UBQLN2-MBP protein emerged in the flow through and was not recovered in the imidazole eluates (Fig 7A). By contrast, both the GST- and His-tagged WT-UBQLN2 proteins had the opposite profile, being predominantly eluted by imidazole and absent from the flow-through (Fig 7A and B). Their identity was confirmed by reaction of the correct size proteins with antibodies specific for each of their tags (Fig 7B). Their coelution could only occur if the two proteins were bound together in a complex, allowing the capture of each of them by the successive affinity of their tags (see Fig S5). The recovery of only two of the three tagged UBQLN2 proteins after passage over the two columns strongly suggests that the variably-tagged WT-UBQLN2 formed dimers, and not trimers. As a result, passing the protein mixture over GST- then Ni-NTA agarose would capture GST-UBQLN2 bound with His-UBQLN2, but not with MBP-UBQLN2 protein (See Fig S6A). Unexpectedly, estimation of the ratio of the two proteins in the final eluate by their common reaction with the anti-UBQLN2 antibody revealed a 1:2 ratio, and not 1:1, which would be expected if they only bound together as a dimer (Fig 7C). Nevertheless, the data strongly suggests WT-UBQLN2 can dimerize with itself.

We repeated the assay to determine if mutant UBQLN2 carrying the P497S mutation can bind WT-UBQLN2. The same proteins and pulldown strategy were used except that GST-P497S-UBQLN2 was substituted for GST-WT-UBQLN2. Like before all three proteins were detected in the starting mixture, and only GST-P497S-UBQLN2 and His-WT-UBQLN2, but not MBP-WT-UBQLN2 were recovered from the eluted Ni-NTA column (Fig 7D). These results indicate that UBQLN2 proteins carrying the P497S mutation can form dimers with WT-UBQLN2 too.

Finally, we examined whether WT and P497S mutant UBQLN2 proteins bind UBQLN1 by a similar assay. Accordingly, similar amounts of GST-WT-UBQLN1 were mixed with either His-WT-UBQLN2 or His-P497S-UBQLN2 proteins and the mixture was applied onto Ni-NTA beads. Examination of the flow through and imidazole eluates from the column with an anti-GST antibody revealed similar recovery of GST-UBQLN1 from both the His-WT and His-P497S UBQLN2 mixtures (Fig 7E and S6A). A reprobe of the same blot with an anti-UBQLN2 antibody revealed recovery of the two different HIS-UBQLN2 proteins from the columns, as expected. The signal from the anti-GST incubation still remained, but was useful to distinguish the position of the HIS-tagged UBQLN2 proteins in the blots (Fig 7E and S6A). These results indicate that WT and P497S mutant UBQLN2 proteins bind equally well with WT UBQLN1 protein.

DISCUSSION

Here we have presented evidence, based on alterations of its intrinsic Trp fluorescence, that UBQLN2 protein undergoes a significant conformational change upon shifting its incubation temperature from 37°C to 42°C, suggesting that the conformational switch may regulate its function in the heat-shock response. Consistent with this idea, we found that

binding between purified UBQLN2 and HSPA1B proteins is dramatically increased by the change in temperature. Furthermore, restoration of the temperature to 37°C decreased both Trp fluorescence and binding with HSPA1B. By comparison, we found all five ALS/FTD mutant UBQLN2 proteins we tested had significantly attenuated changes in Trp fluorescence compared to WT-UBQLN2, suggesting that the thermo-regulation of the conformational switch is crippled in the mutants. Paradoxically, however, all five mutants bound similar amounts of HSPA1B as WT-UBQLN2 protein at 42°C, suggesting that either the conformational switch is not instrumental for HSPA1B binding or that, although damaged, the switch is still functional. We also found that several of the mutants displayed minor differences in their capacity to bind polyubiquitin chains at the elevated 42°C temperature. Opposite to the effects seen in HSPA1B binding, raising the temperature from 37°C to 42°C slightly decreased K48 and K63 poly-ubiquitin chain binding with UBQLN2, but the difference was not significant. Comparison of the poly-ubiquitin chain binding affinity revealed WT-UBQLN2 binds more avidly with K63 than with K48 chains. The K63 avidity fits well with the functional role ascribed for UBQLN2 in autophagy and cell signaling [9, 24]. Consistent with its known function in autophagy, we found UBQLN2 binds directly with LC3, the autophagosomal-specific membrane-tethered protein, providing a biochemical basis for how UBQLN2 may get recruited to autophagosomes. Finally, we provide evidence that WT-UBQLN2 proteins can homodimerize together, as well as heterodimerize with WT-UBQLN1 protein. We further show that ALS mutant P497S-UBQLN2 protein can dimerize with WT-UBQLN1 and 2 proteins providing a possible mechanism for how dominant mutations in UBQLN2 may bind and deplete the functional UBQLN pool, leading to loss of UBQLN2 function.

We speculate that the conformational switch in UBQLN2 is activated to alter its function. Based on our evidence that the switch is activated by raising the temperature from 37°C to 42°C, this temperature specificity implicates a role in the heat shock response. Consistent with this speculation, UBQLN2 localization is known to change dramatically: from generally more diffuse in cells cultured at 37°C to becoming highly concentrated, discreet puncta in the cytoplasm following exposure to heat shock at 42°C. The puncta have been identified as stress granules (SGs) [15, 25], which are formed rapidly in cells to protect against temperature-induced damage [26]. Thus, we speculate that the temperature-induced conformational switch exposes binding sites in UBQLN2 facilitating its recruitment to stress granules. Although UBQLN2 is known to bind many proteins in SGs [27], we believe that its binding to HSP70 proteins, like HSPA1B, could play an instrumental role in SG targeting. Indeed, SG formation is known to be regulated by HSP70 [28, 29]. The large temperature-induced increase in binding between UBQLN2 and HSPA1B that we found *in vitro* is consistent with increased coimmunoprecipitation of HSP70 proteins with UBQLN2 found in cells cultured at 42°C compared to 37°C [13]. The authors of that study found more polyubiquitinated proteins were coimmunoprecipitated at the higher temperature, but could not resolve whether the increase in HSP70 coimmunoprecipitation was due to direct binding with UBQLN2 or indirectly associated through the UBA-bound misfolded polyubiquitinated proteins. Here, we have demonstrated that UBQLN2 binds directly with HSP70, independent of any binding to the misfolded proteins. The HSP70 binding sites in UBQLN2 were recently mapped to its STI domains, consistent with the HSP70-binding

property of such domains [11, 17, 30]. To explain our findings, we therefore predict that the STI1 domains in UBQLN2 are normally buried in cells cultured at 37°C, which precludes interaction with HSPA1B, but the conformational change triggered by temperature elevation leads to exposure of the STI1 domains, allowing for HSPA1B interaction. Based on this model, we propose that UBQLN2 may be a sensor in the heat shock response. It will be interesting to determine if other cellular stressors besides heat shock also activate the conformational change in UBQLN2.

Interestingly, we mapped the UBQLN2 binding site in HSPA1B to the ATP binding domain and not the peptide binding domain, which is typically involved in protein refolding. We speculate that the mode of interaction may free HSPA1B's peptide binding domain to interact with misfolded proteins, which are captured through interaction of their polyubiquitin chains to the UBA domain of UBQLN2.

Previous studies had shown reduced HSP70 coimmunoprecipitation with several ALS mutant UBQLN2 proteins, speculating that the decrease may be responsible for reduced chaperone binding and aggregate clearance [13, 14, 17]. Unexpectedly, we found no major difference in the magnitude of the temperature-induced increase in HSPA1B direct binding with any of the 5 ALS UBQLN2 mutants we tested. The reason why we failed to detect a difference in HSPA1B binding with the mutants is not clear, despite finding that they were all defective in the conformational switch. More detailed investigation is needed to resolve the discrepancy and to determine whether the effects seen in cells arise due to a subtle conformational change that is not detectable in our assays or if it occurs for other reasons. It is also possible that factors present in cells may affect HSP70 binding to UBQLN2, which would be absent from our assays. Alternatively, it is also possible that ALS mutations in UBQLN2 may not directly affect the temperature-induced increase in HSP70 binding, like we have shown here, but could nevertheless affect HSPA1B binding through other mechanisms. Interestingly, both WT and ALS mutant UBQLN2 proteins have been shown to localize equally well with SG [27], which is consistent with our findings. Finally, it is possible that a temperature-induced conformational change in HSPA1B itself regulates binding with UBQLN2. However, this binding must be selective for UBQLN2 as little change in binding was observed with GST alone.

The stronger binding affinity of UBQLN2 for K63 compared to K48 ubiquitin chains suggests UBQLN2 plays an important role in pathways that utilize K63 chain linkage. While the rules that govern the choice between different ubiquitin chain linkages are difficult to comprehend, because of their overlapping functions and existence of mixed (heterotypic) ubiquitin linkages, certain general principles are known about the appendage of K63 chains, primary their involvement in autophagy, DNA damage response and NF-κB signaling (reviewed [31, 32]). Consistent with its strong interaction with K63 chains, KO or overexpression of ALS mutant UBQLN2 proteins in animals lead to major disturbances in pathways associated with usage of K63-associated pathways, particularly autophagy and NF-κB signaling [9, 24, 33, 34]. Interestingly we previously found UBQLN1 also displays increased avidity for K63 chains over K48 chains. Taken together, these data strongly imply that the in-vitro binding preference of UBQLN1 and 2 that we found for K63 chains over K48 chains may have physiologic relevance.

Our ubiquitin pulldown experiments clearly revealed that UBQLN2 binds preferentially with K48 and K63 polyubiquitin chains composed of four or more ubiquitin moieties compared to three or fewer ubiquitin moieties (Fig 5A). This preference may be instructive in understanding the functional role played by UBQLN2 relative to the ubiquitin code used in cells [23]. The binding to the longer chains is consistent with usage of longer chains in both protein degradation and signaling pathways, as already mentioned. At the time of this submission Dao et al. [35] reported that UBQLN2 binds single and tetra K48 and K63 ubiquitin chains with similar specificity, although in some assays they found stronger binding with K63 chains. They showed that addition of the different ubiquitin moieties differentially affected phase separation of UBQLN2 *in vitro.* Unfortunately, they did not examine the effects of ubiquitin chains with longer than four ubiquitin moieties, which we found are favored in binding UBQLN2. Our results suggest that examining the effects upon addition of longer ubiquitin chains on the phase separation properties of UBQLN2 could be particularly instructive.

The weaker binding of UBQLN2 with K48 ubiquitin chains compared to K63 chains suggests UBQLN2 may be more “tuned” in responding to K63 ubiquitin chain appendages over K48 appendages, the latter of which is typically tagged onto proteins meant for proteasomal degradation. We should note that this weaker preference does not preclude involvement in proteasomal degradation. In fact, expression of mutant UBQLN2 proteins are known to stall degradation of proteasomal substrates, suggesting the K48 chain binding may have physiologic relevance [1, 13, 16, 18, 36]. The slightly stronger binding of K48 chains with the P506T mutant at 42°C may compound a problem, in light of our previous finding, that the primary defect of the ALS mutants may be in docking with the proteasome and not in ubiquitin binding [18], although defective proteasome function has also been proposed as another reason [37]. Interestingly, the P506T UBQLN2 mutant that displayed strongest binding with K48 chains, and which retained higher binding at 42°C, is the same mutant that we previously found coimmunoprecipitated more ubiquitinated proteins from cells [18]. If our hypothesis is correct, then the failure of the mutants to deliver their bound K48-poly-ubiquitinated protein cargo could result in a build-up of the misfolded proteins, thereby increasing their propensity to aggregate. Indeed, carriers of the P506T mutation have unusually high density of UBQLN2 aggregates in the hippocampus compared to other UBQLN2 mutations [1,9].

Our results showing that UBQLN2 binds directly with LC3 resolves a previously unknown question as to how UBQLN2 gets recruited to autophagosomes. We previously showed that UBQLN2 interacts with LC3 through binding of two complementary portions of the Venus fluorescent protein that were fused onto UBQLN2 and LC3 [9]. Their complementation generated Venus fluorescence in puncta which we showed were autophagosomes. However, the biochemical forces that drive the complementation, besides affinity of the two Venus portions, was not known. Our new findings that UBQLN2 and LC3 proteins bind directly to one another provides a better understanding for the biochemical basis of the complementation. Although UBQLN2 lacks a classic LC3 interacting region (LIR) [38, 39], it has an LIR which is very similar to the LIR in p62. It is likely that this region is the site for LC3 interaction, but further studies are need to confirm its identity.

Our results of the sequential pulldown of different tags that were fused onto UBQLN2 revealed that WT-UBQLN2 can homodimerize as well heterodimerize with the P497S-UBQLN2 mutant protein. Besides the dimers, we found no evidence that UBQLN2 forms trimers. The existence of UBQLN2 in dimers was proposed previously based on calculation of their separation by buoyant density ultracentrifugation and the molecular weight estimation of its size by gel exclusion chromatography [13, 25]. However, UBQLN2 was also reported to form trimers by these assays. The reason why we did not detect its binding in trimers in our assays is not clear. It is possible that the large MBP tag used to tag the protein may have hindered UBQLN2 oligomerization. Nevertheless, our demonstration that UBQLN2 forms dimers is instructive as it could help explain how mutant UBQLN2 protein can bind and inactivate UBQLN proteins from cells. We hypothesize, based on our *in vitro* binding fndings, that dimerization of mutant UBQLN2 with WT-UBQLN1 and/or WT UBQLN2 in cells could lead to sequestration of the proteins from the functional pool in cells, leading to the loss of UBQLN function. Interestingly, we and others previously reported that UBQLN1 can form dimers and that the central domain that contains the STI1 domains is responsible for the dimerization [40, 41].

The temperature-induced conformational change we found in UBQLN2 suggests its structure is finely tuned to sense a temperature change of 5°C. Besides the structural change found here, UBQLN2 proteins are known to be highly dynamic, including being able to phase separate into membrane-less organelles depending on culture conditions [15, 27, 42, 43]. The ability of the protein to undergo such delicate and dramatic physiochemical structural alterations implies heavy reliance on the integrity of its protein sequence. It is perhaps not surprising that most UBQLN2 mutations are missense mutations, as major alterations in its sequence may “lock” the protein, thereby destroying its flexibility. It will be fascinating to learn how alterations in UBQLN2’s structure regulates its function and how mutations perturb the dynamics and may cause disease.

Supplementary Material

Refer to Web version on PubMed Central for supplementary material.

Acknowledgements

We thank Josephine Wu and Jessie Greenslade for generating the UBQLN2-His and His-LC3B expression constructs, respectively. We thank Dr. Dudley Strickland for allowing us to use the CD equipment for the studies and Victoria Collis for helpful comments on the manuscript.

Funding Acknowledgment

This work was supported by – NIH grants RF1NS098243 and R01NS100008 from the National Institute for Neurological Disorders and Stroke, the National Institute on Aging and the Robert Packard Center for ALS research at Johns Hopkins University – to MJM.

Availability of Data

All the data used for the study is contained in the article or files in the supplemental information. All other datasets used in the study are available from the corresponding author.

References

[1]. Deng HX, Chen W, Hong ST, Boycott KM, Gorrie GH, Siddique N, Yang Y, Fecto F, Shi Y, Zhai H, Jiang H, Hirano M, Rampersaud E, Jansen GH, Donkervoort S, Bigio EH, Brooks BR, Ajroud K, Sufit RL, Haines JL, Mugnaini E, Pericak-Vance MA, Siddique T, Mutations in UBQLN2 cause dominant X-linked juvenile and adult-onset ALS and ALS/dementia, Nature 477(7363) (2011) 211–5. [PubMed: 21857683]

[2]. Higgins N, Lin B, Monteiro MJ, Lou Gehrig's Disease (ALS): UBQLN2 Mutations Strike Out of Phase, Structure 27(6) (2019) 879–881. [PubMed: 31167121]

[3]. Lin BC, Higgins NR, Phung TH, Monteiro MJ, UBQLN proteins in health and disease with a focus on UBQLN2 in ALS/FTD, FEBS J (2021).

[4]. Marin I, The ubiquilin gene family: evolutionary patterns and functional insights, BMC Evol Biol 14 (2014) 63. [PubMed: 24674348]

[5]. Lin BC, Phung TH, Higgins NR, Greenslade JE, Prado MA, Finley D, Karbowski M, Polster BM, Monteiro MJ, ALS/FTD mutations in UBQLN2 are linked to mitochondrial dysfunction through loss-of-function in mitochondrial protein import, Hum Mol Genet 30(13) (2021) 1230–1246. [PubMed: 33891006]

[6]. N'Diaye EN, Kajihara KK, Hsieh I, Morisaki H, Debnath J, Brown EJ, PLIC proteins or ubiquilins regulate autophagy-dependent cell survival during nutrient starvation, EMBO Rep 10(2) (2009) 173–9. [PubMed: 19148225]

[7]. Rothenberg C, Srinivasan D, Mah L, Kaushik S, Peterhoff CM, Ugolino J, Fang S, Cuervo AM, Nixon RA, Monteiro MJ, Ubiquilin functions in autophagy and is degraded by chaperone-mediated autophagy, Hum Mol Genet 19(16) (2010) 3219–32. [PubMed: 20529957]

[8]. Senturk M, Lin G, Zuo Z, Mao D, Watson E, Mikos AG, Bellen HJ, Ubiquilins regulate autophagic flux through mTOR signalling and lysosomal acidification, Nat Cell Biol 21(3) (2019) 384–396. [PubMed: 30804504]

[9]. Wu JJ, Cai A, Greenslade JE, Higgins NR, Fan C, Le NTT, Tatman M, Whiteley AM, Prado MA, Dieriks BV, Curtis MA, Shaw CE, Siddique T, Faull RLM, Scotter EL, Finley D, Monteiro MJ, ALS/FTD mutations in UBQLN2 impede autophagy by reducing autophagosome acidification through loss of function, Proc Natl Acad Sci U S A 117(26) (2020) 15230–15241. [PubMed: 32513711]

[10]. Lee DY, Arnott D, Brown EJ, Ubiquilin4 is an adaptor protein that recruits Ubiquilin1 to the autophagy machinery, EMBO Rep 14(4) (2013) 373–81. [PubMed: 23459205]

[11]. Kaye FJ, Modi S, Ivanovska I, Koonin EV, Thress K, Kubo A, Kornbluth S, Rose MD, A family of ubiquitin-like proteins binds the ATPase domain of Hsp70-like Stch, FEBS Lett 467(2-3) (2000) 348–55. [PubMed: 10675567]

[12]. Bukau B, Horwich AL, The Hsp70 and Hsp60 chaperone machines, Cell 92(3) (1998) 351–66. [PubMed: 9476895]

[13]. Hjerpe R, Bett JS, Keuss MJ, Solovyova A, McWilliams TG, Johnson C, Sahu I, Varghese J, Wood N, Wightman M, Osborne G, Bates GP, Glickman MH, Trost M, Knebel A, Marchesi F, Kurz T, UBQLN2 Mediates Autophagy-Independent Protein Aggregate Clearance by the Proteasome, Cell 166(4) (2016) 935–49. [PubMed: 27477512]

[14]. Teyssou E, Chartier L, Amador MD, Lam R, Lautrette G, Nicol M, Machat S, Da Barroca S, Moigneu C, Mairey M, Larmonier T, Saker S, Dussert C, Forlani S, Fontaine B, Seilhean D, Bohl D, Boillee S, Meininger V, Couratier P, Salachas F, Stevanin G, Millecamps S, Novel UBQLN2 mutations linked to amyotrophic lateral sclerosis and atypical hereditary spastic paraplegia phenotype through defective HSP70-mediated proteolysis, Neurobiol Aging 58 (2017) 239 e11–239 e20.

[15]. Alexander EJ, Ghanbari Niaki A, Zhang T, Sarkar J, Liu Y, Nirujogi RS, Pandey A, Myong S, Wang J, Ubiquilin 2 modulates ALS/FTD-linked FUS-RNA complex dynamics and stress granule formation, Proc Natl Acad Sci U S A 115(49) (2018) E11485–E11494. [PubMed: 30442662]

[16]. Gavriilidis C, Laredj L, Solinhac R, Messaddeq N, Viaud J, Laporte J, Sumara I, Hnia K, The MTM1-UBQLN2-HSP complex mediates degradation of misfolded intermediate filaments in skeletal muscle, Nat Cell Biol 20(2) (2018) 198–210. [PubMed: 29358706]

[17]. Zhang K, Wang A, Zhong K, Qi S, Wei C, Shu X, Tu WY, Xu W, Xia C, Xiao Y, Chen A, Bai L, Zhang J, Luo B, Wang W, Shen C, UBQLN2-HSP70 axis reduces poly-Gly-Ala aggregates and alleviates behavioral defects in the C9ORF72 animal model, Neuron 109(12) (2021) 1949–1962 e6. [PubMed: 33991504]

[18]. Chang L, Monteiro MJ, Defective Proteasome Delivery of Polyubiquitinated Proteins by Ubiquilin-2 Proteins Containing ALS Mutations, PLoS One 10(6) (2015) e0130162. [PubMed: 26075709]

[19]. Monteiro MJ, Mical TI, Resolution of kinase activities during the HeLa cell cycle: identification of kinases with cyclic activities, Exp Cell Res 223(2) (1996) 443–51. [PubMed: 8601422]

[20]. Mayer MP, Recruitment of Hsp70 chaperones: a crucial part of viral survival strategies, Rev Physiol Biochem Pharmacol 153 (2005) 1–46. [PubMed: 15243813]

[21]. Harman CA, Monteiro MJ, The specificity of ubiquitin binding to ubiquilin-1 is regulated by sequences besides its UBA domain, Biochim Biophys Acta Gen Subj 1863(10) (2019) 1568–1574. [PubMed: 31175912]

[22]. Komander D, Rape M, The ubiquitin code, Annu Rev Biochem 81 (2012) 203–29. [PubMed: 22524316]

[23]. Akutsu M, Dikic I, Bremm A, Ubiquitin chain diversity at a glance, J Cell Sci 129(5) (2016) 875–80. [PubMed: 26906419]

[24]. Whiteley AM, Prado MA, de Poot SAH, Paulo JA, Ashton M, Dominguez S, Weber M, Ngu H, Szpyt J, Jedrychowski MP, Easton A, Gygi SP, Kurz T, Monteiro MJ, Brown EJ, Finley D, Global proteomics of Ubqln2-based murine models of ALS, J Biol Chem 296 (2021) 100153. [PubMed: 33277362]

[25]. Dao TP, Martyniak B, Canning AJ, Lei Y, Colicino EG, Cosgrove MS, Hehnly H, Castaneda CA, ALS-Linked Mutations Affect UBQLN2 Oligomerization and Phase Separation in a Position- and Amino Acid-Dependent Manner, Structure 27(6) (2019) 937–951 e5. [PubMed: 30982635]

[26]. Ivanov P, Kedersha N, Anderson P, Stress Granules and Processing Bodies in Translational Control, Cold Spring Harb Perspect Biol 11(5) (2019).

[27]. Peng G, Gu A, Niu H, Chen L, Chen Y, Zhou M, Zhang Y, Liu J, Cai L, Liang D, Liu X, Liu M, Amyotrophic lateral sclerosis (ALS) linked mutation in Ubiquilin 2 affects stress granule assembly via TIA-1, CNS Neurosci Ther 28(1) (2022) 105–115. [PubMed: 34750982]

[28]. Gilks N, Kedersha N, Ayodele M, Shen L, Stoecklin G, Dember LM, Anderson P, Stress granule assembly is mediated by prion-like aggregation of TIA-1, Mol Biol Cell 15(12) (2004) 5383–98. [PubMed: 15371533]

[29]. Mateju D, Franzmann TM, Patel A, Kopach A, Boczek EE, Maharana S, Lee HO, Carra S, Hyman AA, Alberti S, An aberrant phase transition of stress granules triggered by misfolded protein and prevented by chaperone function, EMBO J 36(12) (2017) 1669–1687. [PubMed: 28377462]

[30]. Fry MY, Saladi SM, Clemons WM Jr., The STI1-domain is a flexible alpha-helical fold with a hydrophobic groove, Protein Sci 30(4) (2021) 882–898. [PubMed: 33620121]

[31]. Silva GM, Finley D, Vogel C, K63 polyubiquitination is a new modulator of the oxidative stress response, Nat Struct Mol Biol 22(2) (2015) 116–23. [PubMed: 25622294]

[32]. French ME, Koehler CF, Hunter T, Emerging functions of branched ubiquitin chains, Cell Discov 7(1) (2021) 6. [PubMed: 33495455]

[33]. Picher-Martel V, Dutta K, Phaneuf D, Sobue G, Julien JP, Ubiquilin-2 drives NF-kappaB activity and cytosolic TDP-43 aggregation in neuronal cells, Mol Brain 8(1) (2015) 71. [PubMed: 26521126]

[34]. Osaka M, Ito D, Suzuki N, Disturbance of proteasomal and autophagic protein degradation pathways by amyotrophic lateral sclerosis-linked mutations in ubiquilin 2, Biochem Biophys Res Commun 472(2) (2016) 324–31. [PubMed: 26944018]

[35]. Dao TP, Yang Y, Presti MF, Cosgrove MS, Hopkins JB, Ma W, Loh SN, Castaneda CA, Mechanistic insights into enhancement or inhibition of phase separation by different polyubiquitin chains, EMBO Rep 23(8) (2022) e55056. [PubMed: 35762418]

[36]. Gorrie GH, Fecto F, Radzicki D, Weiss C, Shi Y, Dong H, Zhai H, Fu R, Liu E, Li S, Arrat H, Bigio EH, Disterhoft JF, Martina M, Mugnaini E, Siddique T, Deng HX, Dendritic spinopathy in transgenic mice expressing ALS/dementia-linked mutant UBQLN2, Proc Natl Acad Sci U S A 111(40) (2014) 14524–9. [PubMed: 25246588]

[37]. Zhang W, Huang B, Gao L, Huang C, Impaired 26S Proteasome Assembly Precedes Neuronal Loss in Mutant UBQLN2 Rats, Int J Mol Sci 22(9) (2021).

[38]. Pankiv S, Clausen TH, Lamark T, Brech A, Bruun JA, Outzen H, Overvatn A, Bjorkoy G, Johansen T, p62/SQSTM1 binds directly to Atg8/LC3 to facilitate degradation of ubiquitinated protein aggregates by autophagy, J Biol Chem 282(33) (2007) 24131–45. [PubMed: 17580304]

[39]. Birgisdottir AB, Lamark T, Johansen T, The LIR motif - crucial for selective autophagy, J Cell Sci 126(Pt 15) (2013) 3237–47. [PubMed: 23908376]

[40]. Ford DL, Monteiro MJ, Dimerization of ubiquilin is dependent upon the central region of the protein: evidence that the monomer, but not the dimer, is involved in binding presenilins, Biochem J 399(3) (2006) 397–404. [PubMed: 16813565]

[41]. Kurlawala Z, Shah PP, Shah C, Beverly LJ, The STI and UBA Domains of UBQLN1 Are Critical Determinants of Substrate Interaction and Proteostasis, J Cell Biochem 118(8) (2017) 2261–2270. [PubMed: 28075048]

[42]. Dao TP, Kolaitis RM, Kim HJ, O'Donovan K, Martyniak B, Colicino E, Hehnly H, Taylor JP, Castaneda CA, Ubiquitin Modulates Liquid-Liquid Phase Separation of UBQLN2 via Disruption of Multivalent Interactions, Mol Cell 69(6) (2018) 965–978 e6. [PubMed: 29526694]

[43]. Gerson JE, Linton H, Xing J, Sutter AB, Kakos FS, Ryou J, Liggans N, Sharkey LM, Safren N, Paulson HL, Ivanova MI, Shared and divergent phase separation and aggregation properties of brain-expressed ubiquilins, Sci Rep 11(1) (2021) 287. [PubMed: 33431932]

- Heat shock triggers a conformational switch in UBQLN2
- ALS/FTD mutations in UBQLN2 are crippled in the conformational switch
- Heat shock increases direct binding between UBQLN2 and HSP70
- UBQLN2 binds preferentially with K63 polyubiquitin chains
- UBQLN2 binds directly with LC3
- UBQLN2 homodimerizes and heterodimerizes with UBQLN1

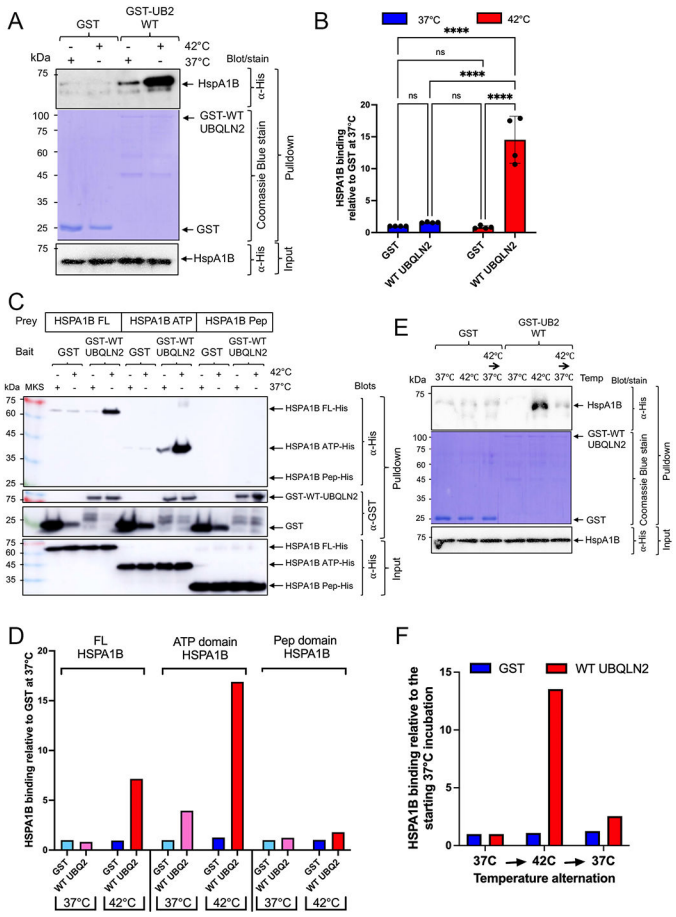

Fig 1.

Reversible temperature-induced binding of HSPA1B with UBQLN2. (A) GST pulldown assay showing that increasing the temperature of incubation from 37°C to 42°C promotes HSPA1B-His binding with GST-UBQLN2 (GST-UB2). (B) Quantification of the change in HSPA1B binding with the GST proteins shown in A. ****$P < 0.0001$. (C) Pulldown assays similar to A, but including assessment of binding to the ATP and Pep binding portions of HSPA1B. (D) Quantification of the binding shown in E.

(E) Similar to A, but including a set of incubations were the temperature was changed from 42°C back to 37°C. (F) Quantification of the results shown in C.

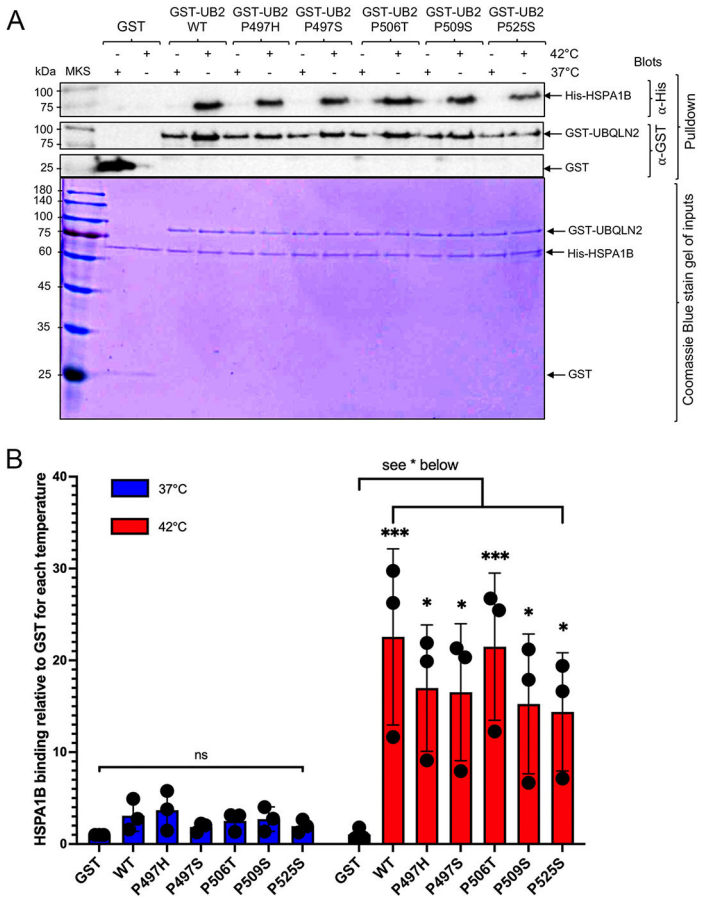

Fig 2.

UBQLN2 fusion proteins carrying ALS/FTD mutations have similar temperature-induced increase in HSPA1B binding as WT-UBQLN2. (A) GST pulldown assays conducted at 37°C and 42°C for GST and GST-UBQLN2 fusion proteins encoding either WT-UBQLN2 or carrying one of five different ALS/FTD mutations. Upper three panels are the blots of the pulldown assays, whereas the lower panel shows the Coomassie Blue stained gel of the beginning protein mixture before the pulldown. (B) Quantification of HSPA1B pulldown relative to GST alone for the two temperature incubations. Increased binding of HSPA1B was seen with all the GST-UBQLN2 fusion proteins, including all five mutants at 42°C compared with GST alone. *$P < 0.05$, ***$P < 0.001$, ns = non-significant. There was no difference in HSPA1B binding with any of the mutants compared to WT-UBQLN2.

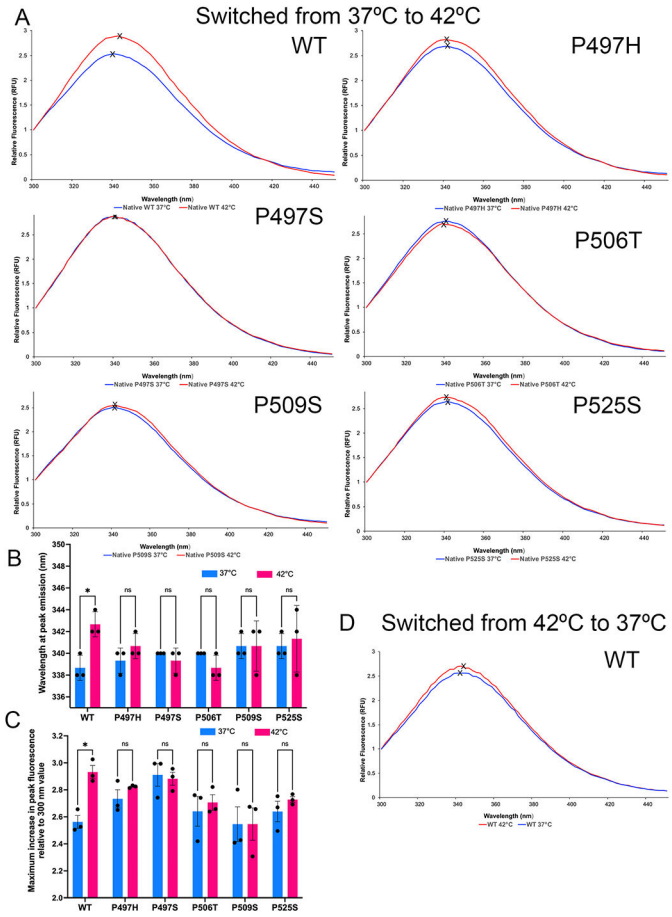

Fig 3.

Comparison of the temperature induced spectral change in tryptophan fluorescence for His-tagged WT and ALS mutant UBQLN2 proteins. The tryptophan emission spectra from 300 to 450 nm produced for each protein at fixed excitation of 270 nm when incubated at 37°C (blue line) and 42°C (red line) are shown (average of three readings). (B and C) Graphical presentation of the wavelength of peak tryptophan fluorescence (B) and maximum alteration in the fluorescence intensity (C) for WT and ALS/FTD mutant UBQLN2 proteins for the 37°C (blue bars) and 42°C (red bars) incubations. $*P < 0.05$, ns = non-significant.

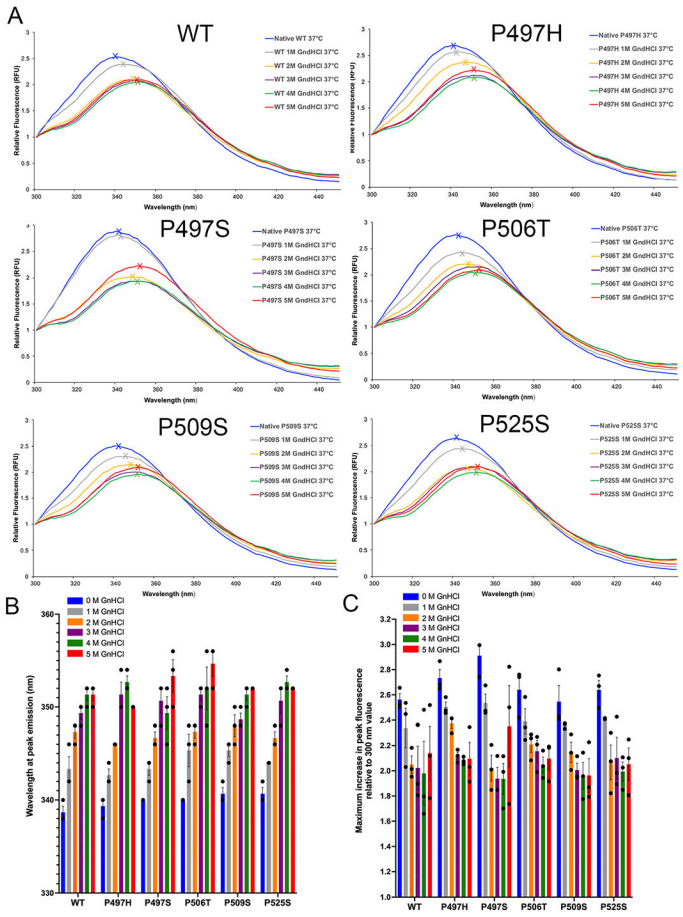

Fig 4.

Comparison of the spectral change in tryptophan fluorescence for His-tagged WT and ALS mutant UBQLN2 proteins after incubation with different concentrations of GndHCl. (A) Spectral scans (average of three) for the different UBQLN2 proteins incubated in progressive increasing GndHCl concentrations from 0 to 5M. (B and C) Graphical presentation of the wavelength of peak tryptophan fluorescence (B) and maximum alteration in the fluorescence intensity (C) for WT and ALS/FTD mutant UBQLN2 proteins shown in A. No significant difference was seen for any of the mutants compared to WT UBQLN2 for any individual GndHCl concentration.

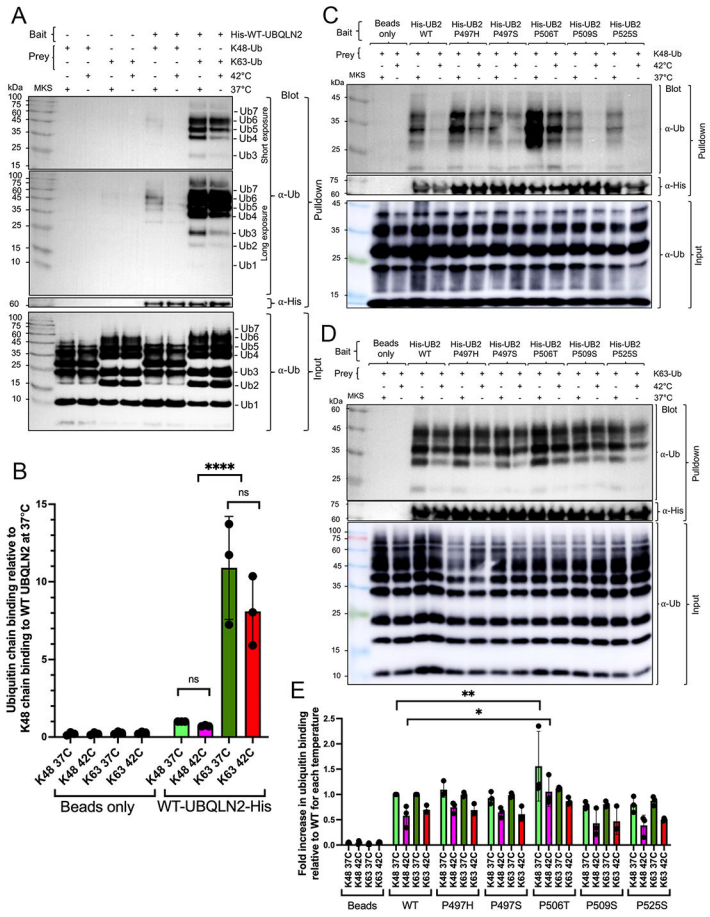

Fig 5.

UBQLN2 binds preferentially with K63 ubiquitin chains than with K48 chains. (A) Blots of the His-UBQLN2 pulldown experiments showing increased binding of WT-UBQLN2 with K63 polyubiquitin chains at 37°C and 42°C. (B) Quantification of K48 and K63 polyubiquitin chain binding with His-tagged WT-UBQLN2 at 37°C and 42°C. (C, D) Blots comparing the pulldown of K48 (C) and K63 (D) polyubiquitin chains at 37°C and 42°C by WT and ALS/FTD mutant His-tagged UBQLN2 proteins. (E) Quantification of the level of K48 and K63 ubiquitin chain binding for different UBQLN2 proteins normalized to the amount of binding seen with WT-UBQLN2 protein at 37°C.

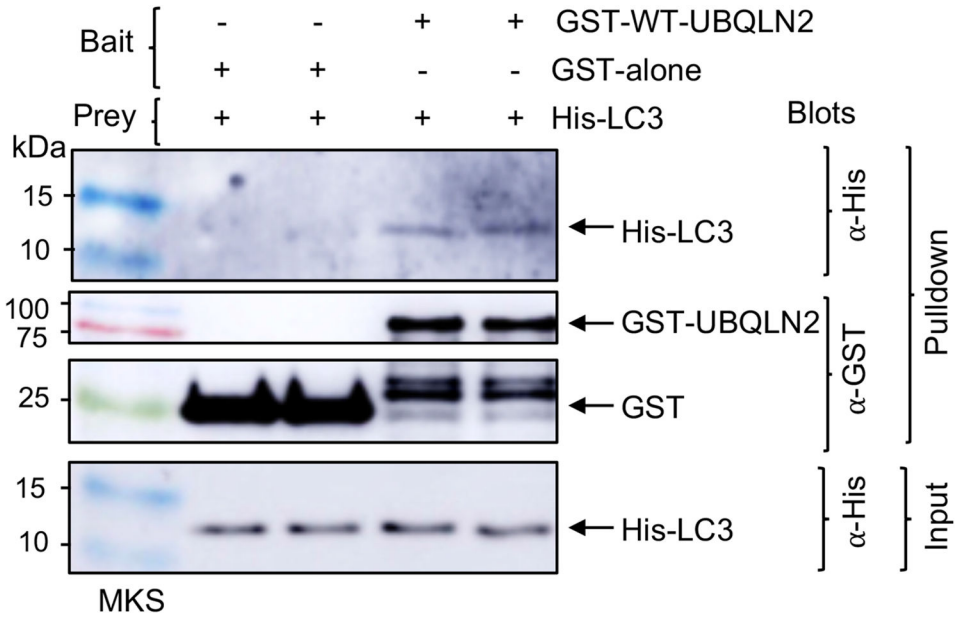

Fig 6.

UBQLN2 binds directly with LC3. GST pulldown assay of duplicate mixtures assessed for UBQLN2 binding to His-tagged LC3 protein. Equal amounts of His-LC3 (prey) was mixed with either GST alone or GST-WT UBQLN2 (bait), in duplicate GST-agarose-binding assays. The beads were washed and the protein that bound to the beads were assayed by immunoblotting with the antibodies shown. The lower panel shows a blot of an aliquot that was saved from the mixtures and probed for His-LC3 protein, showing approximately equal amount of prey that was contained in all the reactions.

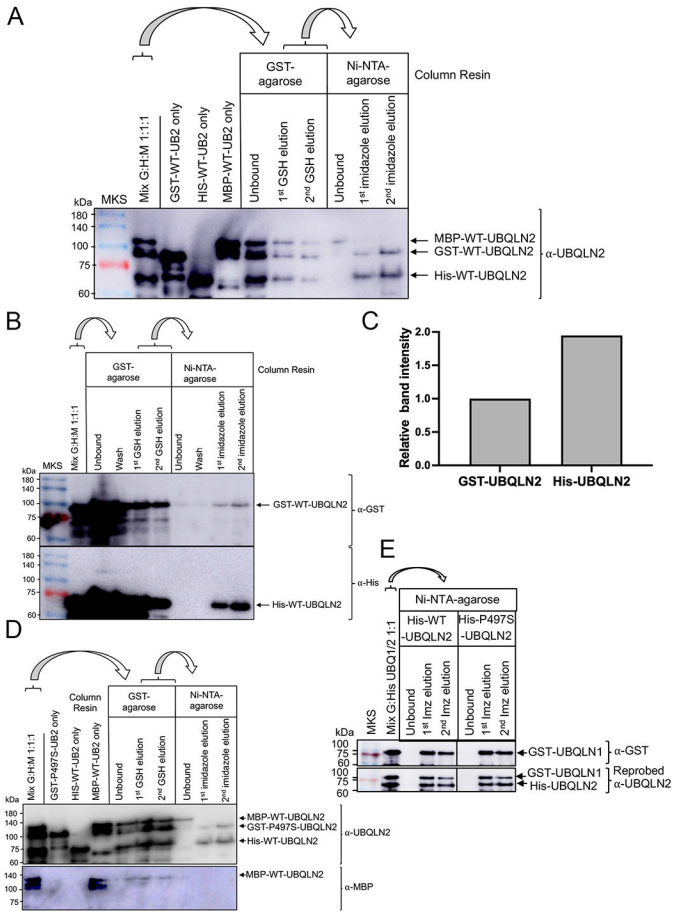

Fig 7.

Sequential pulldown assays reveal UBQLN2 can homo-oligomerize as well as hetero-oligomerize with UBQLN1. (A) Sequential pulldown assay in which approximately equimolar amounts of MBP-, GST- and His-tagged WT-UBQLN2 proteins were first mixed together and then used for two sequential pulldown assays. In the first pulldown the protein mixture was applied over a GST-agarose column to bind GST-UBQLN2 protein. The column was then washed and the bound proteins were eluted with glutathione (GSH). The glutathione-eluted fractions were pooled and applied onto the second Ni-NTA agarose column to bind His-tagged UBQLN2, which was presumably co-eluted from the first column by interaction with GST-UBQLN2. After washing, the bound proteins were eluted with imidazole. The anti-UBQLN2 blots show detection of all three UBQLN2-tagged proteins (MBP-, GST-, and His-) before and after mixing and following binding and elution from representative fractions from the two columns. (B) Representative fractions from the experiment shown in A, but probed with an anti-GST or anti-His antibody to confirm the presence of the two tagged UBQLN2 proteins. (C) Quantification of the band intensity for the two anti-UBQLN2-reactive bands in the 2nd imidazole elution lane shown in A. (D) Identical experiment to A, except that GST-tagged P497S-UBQLN2 was used instead of WT-UBQLN2. Upper panel blotted with an anti-UBQLN2 antibody, showing detection of proteins corresponding to the GST and His-tagged. UBQLN2 proteins. Lower panel is a reprobe for the same blot using an anti-MBP antibody showing failure to detect the protein

in the final imidazole eluates. (E) Mixing experiment in which GST tagged WT-UBQLN1 was mixed with either His-tagged WT-UBQLN2 or P497S mutant UBQLN2 and used for a single Ni-NTA-agarose pulldown assay. The two blots show the mixture (for WT-UBQLN2 proteins with WT UBQLN1) and flow through and imidazole (Imz) fractions recovered from the column and probed for GST (upper panel) and then reprobed with an anti-UBQLN2 antibody (lower panel). Residual reaction with GST-UBQLN1 is still seen in the lower panel, which is useful for distinguishing the two different size tagged proteins.